Particle transport induced by electrostatic wave fluctuations

2015 J. Phys.: Conf. Ser. 641 012006

(http://iopscience.iop.org/1742-6596/641/1/012006)

Journal of Physics: Conference Series **641** (2015) 012006 doi:10.1088/1742-6596/641/1/012006

Particle transport induced by electrostatic wave fluctuations

K C Rosalem[1], M Roberto[1] and I L Caldas[2]
[1] Departamento de Física, Instituto Tecnológico de Aeronáutica, 12228-900, São José dos Campos, SP, Brazil
[2] Instituto de Física, Universidade de São Paulo, 05315-970, São Paulo, SP, Brazil

E-mail: kaue@ita.br

Abstract. Particle transport driven by electrostatic waves at the plasma edge is numerically investigated, for large aspect ratio tokamaks, by considering a kinetic model derived from guiding-center equations of motion. Initially, the transport is estimated for trajectories obtained from differential equations for a wave spectrum generated by a dominant spatial mode and three time modes. Then, in case of infinite time modes, the differential equations of motion are used to introduce a symplectic map that allows to analyze the particle transport. The particle transport barriers are observed for spatial localized dominant perturbation and infinite modes. In presence of infinite spatial modes, periodic islands arise in between chaotic trajectories at the plasma edge.

1. Introduction

Several experiments in tokamaks indicate a broad frequency spectrum of plasma drift waves for each wave number [1-3] and the drift waves show substantial amplitudes that imply chaotic particle trajectories [4-8]. Thus, the drift waves are essential features to properly describe the observed driven turbulent transport. Accordingly, this transport is mainly caused by the particle $\boldsymbol{E} \times \boldsymbol{B}$ drift due to the equilibrium and the perturbing electric fields [9,10] and such transport is much affected by the equilibrium field radial profiles [11-13].

In this work, we integrated numerically particle trajectories to investigate the relation between transport and electrostatic wave fluctuations at the plasma edge for large aspect ratio tokamaks. Initially, we assume different amplitude levels in the wave spectra for three specific time modes. The particle trajectories are obtained by integrating differential equations. Complementary, to investigate infinite mode perturbations, these equations of motion are rewritten as a symplectic map in which all modes have the same amplitude.

Early works on electrostatic wave fluctuations derive a drift wave maps around the radial position associated to the minimum of safety factor profiles [4-6]. However, the confined particles can leave the neighborhoods of this minimum point for long time integration. Avoiding this radial limitation, we show how the transport is affected by changing the shear of the radial electric and poloidal magnetic fields [14]. To describe drift waves in tokamak plasmas, the electrostatic spatial modes have to be defined by a dominant perturbations or treat as a generalized modes. Besides, we also study how the particle orbits are modified when the local perturbations are replaced by infinite spatial modes.

In section 2, we introduced the drift-kinetic model that leads to the differential equations for the particle trajectories in the vicinity of a given magnetic and electric field profiles. In section 3, we

[1] To whom any correspondence should be addressed.

compared the Poincaré maps obtained by integrating the drift-kinetic model for specific resonances with the symplectic map for infinite spatial modes. The observed particle transport is summarized and concluded in section 4.

2. Drift-kinetic model

This section provides the model for which the particle trajectories can be calculated in presence of fluctuating electrostatic potential, describing drift waves propagating in the poloidal and toroidal directions according to the spatial modes. For that, we consider the particle trajectories along the magnetic field lines and the displacement due to the drift velocity in the guiding-center equation of motion,

$$\frac{d\boldsymbol{x}}{dt} = v_{\parallel}\frac{\boldsymbol{B}}{B} + \frac{\boldsymbol{E}\times\boldsymbol{B}}{B^2}, \tag{1}$$

where the components of $\boldsymbol{x} = (r, \vartheta, \varphi)$ are defined as the local polar coordinates. Thus, the plasma configuration corresponds to a layer of large aspect ratio tokamak.

The electric field is composed by a fluctuating component $\tilde{\boldsymbol{E}} = -\boldsymbol{\nabla}\tilde{\phi}$ plus an equilibrium radial profile $\boldsymbol{E}_r$, and the magnetic curvature is introduced by the safety factor profile for $B \approx B_{\varphi} \gg B_{\vartheta}$. In order to consider a fluctuating potential in this model we use the wave spectrum,

$$\tilde{\phi}(\boldsymbol{x}, t) = \sum_{m,l,n} \phi_{m,l,n}\, cos(m\vartheta - l\varphi - n\omega_0 t)\,, \tag{2}$$

where $\phi_{m,l,n}$ is the mode amplitude, ω_0 the lowest angular frequency with substantial amplitude in the drift wave spectrum, *m* and *l* define the spatial modes and *n* the time mode in this coordinate system. In the numerical simulations, we assume a dominant *M/L* spatial mode and three harmonics *n* time modes.

We introduce action and angle variables as $I = (r/a)^2$ and $\Psi = M\vartheta - L\varphi$, respectively [5]. Taking these assumptions we obtain the differential equations for the particle trajectories,

$$\frac{dI}{dt} = \frac{2M}{a^2 B}\sum_{M,L,n}^{N} \phi_{m,l,n}\, sin(\Psi - n\omega_0 t)\,, \tag{3}$$

$$\frac{d\Psi}{dt} = \frac{v_{\parallel}}{Rq(I)}[M - Lq(I)] - \frac{ME_r(I)}{aB\sqrt{I}}. \tag{4}$$

To solve this system, the equilibrium fields and the parallel velocity along the magnetic field lines have to be defined for a set tokamak parameters.

3. Transport barrier and diffusion

We investigate numerically the particle transport properties by integrating the equations of motion. Simulations are carried out using the TCABR tokamak parameters, assuming a dominant spatial mode $M/L = 16/4$, particle parallel velocity constant $v_{\parallel} = 1.5\, km\, s^{-1}$ along the trajectories [15] and lowest angular frequency $\omega_0 = 6 \times 10^4\, rad\, s^{-1}$ [3]. For this tokamak configuration we use $R = 61\, cm$, $a = 18\, cm$ and $B = 1.1\, T$. We choose the non-monotonic electric field and monotonic magnetic field profiles discussed in [14].

In order to analyze changes in the radial transport due to the amplitude modes ϕ_{MLn}, we compare the wave spectra for the cases (a) and (b) in figure 1. These perturbing spectra are composed by three time modes n at the plasma edge, whose resonance radial positions can be determined by taking the condition $d/dt\,(\Psi - n\omega_0 t) \cong 0$. In figure 2 we observe the resonance conditions around $n = 3$ with double location for the radial positions.

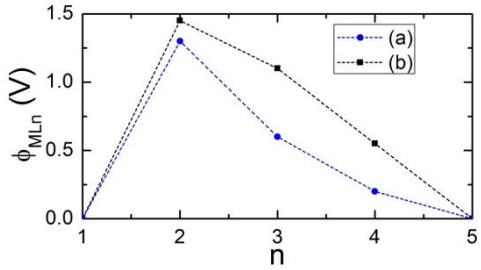

Figure 1. Eletrostatic wave spectra (a) and (b) for a dominant $M/L = 16/4$ spatial mode.

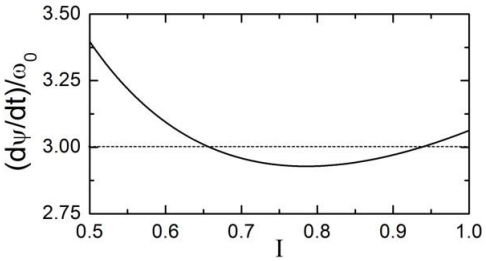

Figure 2. Resonance conditions around $n = 3$ and assuming the lowest angular frequency as $\omega_0 = 6 \times 10^4\ rad\ s^{-1}$ for the cases (a) and (b) in figure 1.

In figure 3(a) we present the Poincaré map obtained by integrating equations (3) and (4) for various initial conditions and assuming the wave spectrum (a) shown in figure 1. The resonance $n = 3$ corresponds to the twin islands separated by the shearless curve depicted in red, which is located by the extremum value of the rotational number profile [14]. In figure 3(b) we assumed the wave spectrum (b) of figure 1, and all the other parameters are the same as those used in the previous map. The onset of meanders [16,17] are induced around of the shearless curve by increasing the wave mode amplitudes. Furthermore, this mode increasing also gives rise to noticeable chaotic trajectories around the inner radial perturbation created by $n = 4$, as seen in figure 3(b). The invariant shearless barrier persists for the modified spectrum.

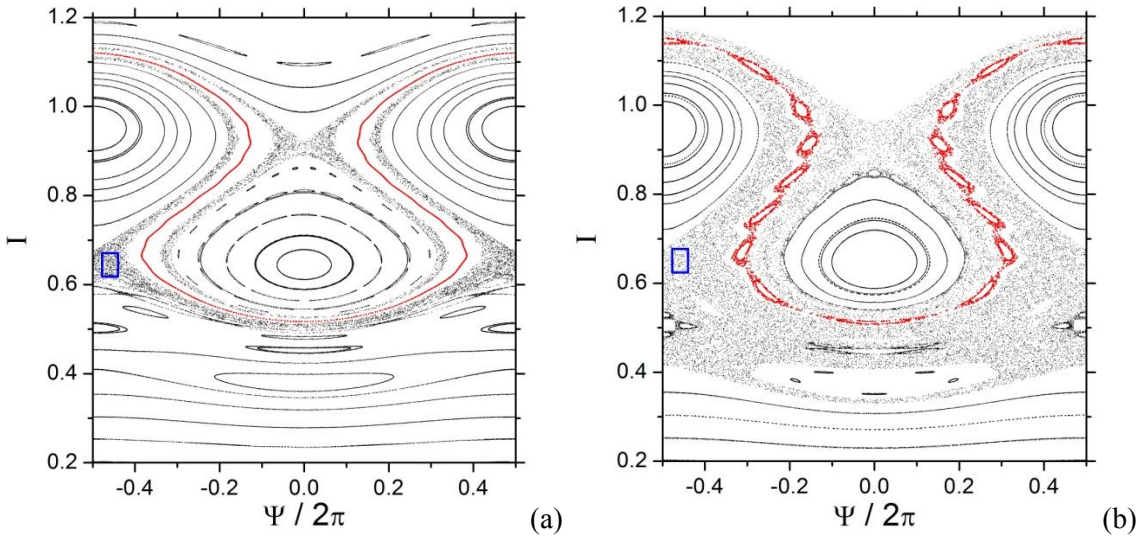

Figure 3. Poincaré maps for the wave spectra (a) and (b) in figure 1. The potential mode amplitudes in case of (a) are $\phi_{MLn=2} = 1.30\ V$, $\phi_{MLn=3} = 0.60\ V$, and $\phi_{MLn=4} = 0.20\ V$, for (b) are $\phi_{MLn=2} = 1.45\ V$, $\phi_{MLn=3} = 1.10\ V$, and $\phi_{MLn=4} = 0.55\ V$. The shearless curves can be identified by the invariant in red. Initial conditions for running diffusion coefficients are shown in the blue grids.

Figure 4 shows the time dependence of the running diffusion coefficient [4] calculated for the particle radial positions for cases (a) and (b) of wave spectra in figure 1. For these calculations, we considered the blue grid in the Poincaré maps of figure 3. One observes the increase of particle transport as increasing the amplitude modes by modifying the wave spectrum.

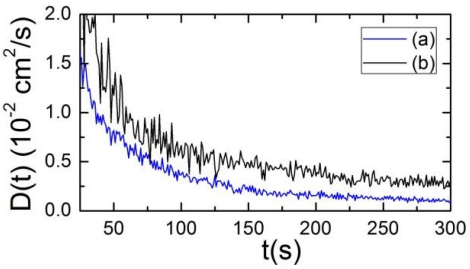

Figure 4. Running diffusion coefficients for the blue grids depicted in figure 3.

Despite this model relates a specific electrostatic amplitude for each time mode, it is limited by the wave spectrum characterized by finite *n* modes. To simulate how a continuum wave spectrum affects the particle transport, a symplectic map is derived for infinite time modes. In this case, one can approach the oscillations sum by considering the delta function and impulsive iterations at time $t = 2\pi n/\omega_0$. Thus, one can rewrite the equations (3) and (4) as a map given by

$$I_{N+1} = I_N + \frac{4\pi M}{\omega_0 a^2 B}\phi_{ML}\, sin(\chi)\,, \tag{5}$$

$$\chi_{N+1} = \chi_N + R_1(I_{N+1}) + R_2(I_{N+1})\,, \tag{6}$$

$$R_1(I) = \frac{v_\parallel}{\omega_0 R q(I)}[M - Lq(I)]\,, \tag{7}$$

$$R_2(I) = -\frac{ME_r(I)}{\omega_0 aB\sqrt{I}}, \tag{8}$$

where the angle variable is defined as $\chi = \Psi/2\pi$.

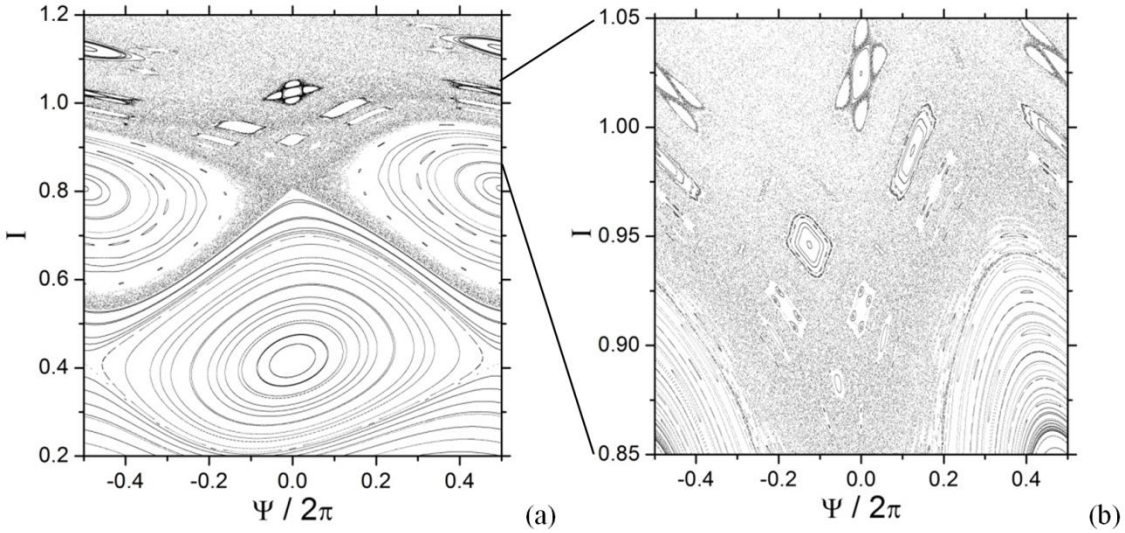

Figure 5. Symplectic map (b) for potential mode amplitude $\phi_{ML} = 0.65\,V$ and (b) the same map amplified at the plasma edge.

In figure 5 we present the symplectic map by using the equations (5) and (6) for various initial conditions and considering the same dominant spatial mode as in figure 3. The symplectic map shows the same structures for particle transport predictions, as seen in figure 5(a). Since the map has infinity time modes at the plasma edge, we expect to identify many islands immersed in a chaotic sea, as it is clearly shown by the amplification in figure 5(b).

4. Conclusions

We have investigated how the particle transport increases with the mode amplitude of the fluctuating electric potential and how this transport changes with the radial field profiles. To analyze this dependence, the running coefficient has been computed and compared for modifications in the drift wave spectrum. We observed in the Poincaré maps robust barriers provided by the electric and magnetic configurations that persist for these spectra. Through the resonance condition, we identified these barriers in between the twin islands region. From the equations of motion we introduced a symplectic map to consider infinite time modes of perturbations. For this map method, we observed many islands where the particles could be trapped along of their trajectories at the plasma edge.

Acknowledgments

This work was supported by São Paulo Research Foundation (FAPESP, Brazil) under Grant No 2013/0340-6 and 2011/19296-1, CNPq and CAPES.

References

[1] Devynck P, Stckel J, Admek J, Duran I, Hron M and Ooost G V 2003 *Czech. J. Phys* **53** 853
[2] Oost G V, Admek J, Antoni V, Balan P, Boedo JA, Devynck P, Duran I, Eliseev L, Gunn J P, Hron M, Ionita C, Jachmich S, Kirnev G S, Martines E, Melnikov A, Schrittwieser R, Silva C, Stöckel J, Tendler M, Varandas C, Schoor M V, Vershkov V, and Weynants R R 2003 *Plasma Phys. Contr. Fusion* **45** 621
[3] Nascimento I C, Kuznetsov Yu K, Guimarães-Filho Z O, Chamaa-Neto I El, Usuriaga O, Fonseca A M M, Galvão R M O, Caldas I L, Severo J H F, Semenov I B, Ribeiro C, Heller M V P, Bellintani V, Elizondo J I, Sanada E 2007 *Nucl. Fusion* **47** 1570
[4] Park H-B, Heo E-G, Horton W, and D-I Choi 1997 *Phys. Plasmas* **4** 3273
[5] Horton W, Park H-B, Kwon J-M, Strozzi D, Morrison P J, and Choi D-I 1998 *Phys. Plasmas* **5** 3910
[6] Kwon J-M, Horton W, Zhu P, Morrison P J, Park H-B, and Choi D-I 2000 *Phys. Plasmas* **7** 1169
[7] Miskane F, Garbet X, Dezairi A, and Saifaoui D 2000 *Phys. Plasmas* **7** 4197
[8] Marcus F A, Caldas I L, Guimarães-Filho Z O, Morrison P J, Horton W, Kuznetsov Y K, and Nascimento I C 2008 *Phys. Plasmas* **15** 112304
[9] Horton W 1999 *Rev. Mod. Phys.* **71** 735
[10] Del-Castillo-Negrete D and Martinelli J J 2012 *Commun. in Nonlinear Sci. and Numer. Simul.* **17** 2031
[11] Ritz C P, Bravenec R V, Schoch P M, Bengtson R D, Boedo J A, Forster J C, Gentle K W, He Y, Hickok R L, Kim Y J, Lin H, Phillips P E, Rhodes T L, Rowan W L, Valanju P M, and Wootton A J. 1989 *Phys. Rev. Lett.* **62** 1844
[12] Hidalgo C, Pedrosa M A, and Gonçalves B 2002 *New J. Phys.* **4** 51
[13] Gürcan Ö D, Garbet X, Hennequin P, Diamond P H, Casati A, and Falchetto G L 2009 *Phys. Rev. Lett.* **102** 255002
[14] Rosalem C K, Roberto M, Caldas I L 2014 *Nucl. Fusion* **54** 064001
[15] Severo J H F, Nascimento I C, Tsypin V S, and Galvão R M O 2003 *Nucl. Fusion* **43** 1047
[16] Caldas I L, Viana R L, Szezech J D r, Portela J S E, Fonseca J, Roberto M, Martins C G L, Silva E J 2012 *Commun. Nonlinear Sci. Numer. Simul.* **17** 2021
[17] Szezech J D Jr, Caldas I L, Lopes S R, Morrison P J, Viana R L 2012 *Phys. Rev. E* **86** 036206